Clinical Neurophysiology 130 (2019) 1243–1252

Contents lists available at ScienceDirect

Clinical Neurophysiology

journal homepage: www.elsevier.com/locate/clinph

Neurophysiological evidence of impaired attention and working memory in untreated hematologic cancer patients

D.E. Anderson [a,b,f,*], V.R. Bhatt [b,c], K. Schmid [d], S.A. Holstein [b,c], M. Lunning [b,c], A.M. Berger [b,e], M. Rizzo [a,b]

[a] Department of Neurological Sciences, College of Medicine, University of Nebraska Medical Center (UNMC), United States
[b] Fred & Pamela Buffett Cancer Center, UNMC, United States
[c] Division of Oncology & Hematology, Department of Internal Medicine, UNMC, United States
[d] Department of Biostatistics, College of Public Health, UNMC, United States
[e] College of Nursing, UNMC, United States
[f] Department of Ophthalmology & Visual Science, College of Medicine, UNMC, United States

ARTICLE INFO

Article history:
Accepted 15 April 2019
Available online 24 May 2019

Keywords:
Attention
Cancer
Cognitive impairment
Electroencephalography
Hematologic cancer
Working memory

HIGHLIGHTS

- This study probed electrophysiological correlates of cognition in hematologic cancer patients.
- Electrophysiology findings showed impaired control over spatial attention and working memory.
- Brain networks governing these functions may be disrupted by hematologic cancer pathophysiology.

ABSTRACT

Objective: Neuroimaging studies of hematologic cancer patients report altered activity in dorsal attention and central executive networks. To determine the consequences of these altered brain networks, we evaluated neurophysiological correlates of attention and working memory in hematologic cancer patients prior to initiating treatment.
Methods: Hematologic cancer patients (19–80 years) were excluded for premorbid cognitive impairment, prior non-hematologic cancer diagnosis, and prior chemotherapy. Attention was manipulated by presenting an irrelevant spatial cue prior to visual search displays. Working memory was manipulated by presenting irrelevant distractors within memory displays. Electroencephalogram was recorded during task performance.
Results: Patients (n = 28) and controls (n = 15) were balanced on age, gender, and education. Spatial cues evoked larger N2pc amplitudes, a correlate of spatial attention, in patients than controls ($p < .05$; Cohen's $d > 0.7$). Memory distractors evoked larger contralateral delay activity amplitudes, a correlate of working memory load, in patients ($p = .028$; Cohen's $d = 1.1$) but not controls ($p = .64$).
Conclusions: Prior to initiating treatment, hematologic cancer patients demonstrated poor control over spatial attention and working memory, consistent with altered dorsal attention and central executive network activity.
Significance: Hematologic cancer patients may be at a higher risk for selecting, processing, and storing distracting information that would compete with more immediate goal-related behaviors.

1. Introduction

Cancer patients are at risk for neurologic complications even in the absence of brain metastases (Bang et al., 2011). Mild cognitive impairment is reportedly present in up to 75% of cancer patients throughout their disease (Janelsins et al., 2014). Despite the prevalence of cognitive changes, subjective reports of cognitive disturbances are weakly related to objective cognitive performance (Hutchinson et al., 2012). One possible explanation for this discrepancy is that subtle cognitive changes in cancer patients may go undetected by neuropsychological measures developed to detect severe functional deficits. Developing more sensitive measures of cognitive impairment may improve detection and management of cognitive symptoms in cancer patients.

* Corresponding author at: Department of Neurological Sciences, University of Nebraska Medical Center, 988440 Nebraska Medical Center, Omaha, NE 68198, United States.
E-mail address: david.anderson@unmc.edu (D.E. Anderson).

https://doi.org/10.1016/j.clinph.2019.04.714
1388-2457/

Few studies have assessed cognitive performance in hematologic cancer patients (Williams et al., 2016), highlighting these patients as an underserved cancer population. Cognitive impairment has been reported in up to 44% of hematologic cancer patients prior to initiating treatment (Hshieh et al., 2018; Meyers et al., 2005). Two cross-sectional positron emission tomography (PET) studies of lymphoma patients demonstrated altered resting-state metabolic activity in dorsal attention network and central executive network (Baudino et al., 2012; D'Agata et al., 2013). Specifically, lower metabolism rates in dorsolateral prefrontal cortex, medial prefrontal cortex, frontal eye fields, precuneus, and superior parietal lobules were associated with greater number of chemotherapy cycles and shorter post-chemotherapy time (Baudino et al., 2012). It remains unclear, however, how altered metabolic activity within dorsal attention and central executive networks is associated with cognitive impairment in hematologic cancer patients.

The goal of the current work was to isolate a core set of impaired cognitive functions in untreated hematologic cancer patients that map onto reported patterns of brain network dysfunction. In non-cancer populations, associations between brain network activity and cognitive performance have been extensively studied. Dorsal attention network activity, which depends on frontal eye fields and intraparietal sulcus (Corbetta and Shulman, 2002; Vossel et al., 2014), has been associated with control over spatial shifts of attention towards distracting stimuli (Capotosto et al., 2009; Ptak and Schnider, 2010). For example, task performance in patients exhibiting greater dorsal attention network dysfunction is more likely to be impaired by an unexpected distracting stimulus. Central executive network activity, which depends on dorsolateral prefrontal cortex and posterior parietal cortex (Sridharan et al., 2008), has been associated with maintaining and manipulating information in working memory (Miller and Cohen, 2001; Müller and Knight, 2006). Based on these findings, we sought to determine whether untreated hematologic cancer patients would show deficits in neurophysiological correlates of: (1) control over spatial shifts of attention; and (2) maintaining and manipulating information in working memory.

We assessed neurophysiological correlates of attention and working memory functions in untreated hematologic cancer patients by recording electroencephalography (EEG) during computer-based task performance. During a modified *visual search task* (Folk et al., 1992; Harris et al., 2017; Theeuwes, 1994), we measured the ability to control involuntary spatial shifts of attention by presenting a task-irrelevant cue immediately prior to the visual search display. EEG waveforms were time-locked to the task-irrelevant cue to measure the N2pc event-related potential (ERP) component (Harris et al., 2017), a phasic negative amplitude deflection in posterior electrodes contralateral to spatial shifts of attention that emerges approximately 200 milliseconds following stimulus presentation (Luck and Hillyard, 1994; Woodman and Luck, 1999). During a modified *change detection task* (Jost et al., 2011; Vogel et al., 2005), we measured the ability to control information content in working memory by presenting task-irrelevant items within memory displays. EEG waveforms were time-locked to memory displays to measure the contralateral delay activity (CDA) ERP component, a sustained negative amplitude modulation in posterior electrodes contralateral to remembered items that emerges approximately 300–400 milliseconds following stimulus presentation (Luria et al., 2016; Vogel and Machizawa, 2004). The CDA was measured to index storage of task-irrelevant items in working memory (Vogel et al., 2005). Together, the N2pc and CDA ERP components offer direct neurophysiological measurements of cognitive processes associated with dorsal attention and central executive networks.

We hypothesized that untreated hematologic cancer patients, relative to healthy controls, would show: (1) larger N2pc amplitudes in response to task-irrelevant cues during the visual search task, which would indicate poor control over spatial shifts of attention; and (2) larger CDA amplitudes in response to memory displays containing task-irrelevant items during the change detection task, which would indicate poor control over manipulating information in working memory. We reasoned that results from this study would provide novel evidence for dorsal attention and central executive network dysfunction that would motivate the development of more sensitive measures of cognitive impairment in hematologic cancer patients.

2. Methods

2.1. Study design and participants

A cross-sectional observational study of hematologic cancer outpatients and healthy control participants was conducted at a tertiary medical center in Omaha, Nebraska between September 2016 and November 2017. Hematologic cancer patients were recruited from the Fred and Pamela Buffett Cancer Center at the University of Nebraska Medical Center (UNMC). Patients were recruited into one of two cohorts based on their treatment plan: (1) scheduled to receive chemotherapy (Ctx+ group); and (2) receiving best support care or undergoing active monitoring (Ctx− group). Inclusion criteria for both groups were: (1) 19–80 years of age, and (2) normal or corrected-to-normal vision. Exclusion criteria for both groups were: (1) previous cancer diagnosis, (2) previous radiotherapy or chemotherapy, and (3) baseline mild cognitive impairment (Mini-Mental State Examination score <25). Study procedures reported here were completed prior to initiating treatment. We recruited a third cohort of healthy controls that were demographically-matched (age:± 5 years; education: ±2 years; gender) to the Ctx+ group. Healthy controls were recruited from an existing research registry in the UNMC Department of Neurological Sciences. All participants provided verbal and written informed consent approved by the UNMC Institutional Review Board and Scientific Review Committee.

2.2. Clinical assessments

Neuropsychological Measures. Four neuropsychological assessments were administered to assess cognitive function: Trail Making Test (Trails A/B) (Lezak, 1995), Golden Stroop (Golden, 1978), Paced Auditory Serial Addition Task (PASAT) (Gronwall and Sampson, 1974), and Useful Field of View (UFOV) (Ball et al., 1988). These assessments measure processing speed (Trails A), attention (PASAT, UFOV), and executive function (Trails B, Stroop). Outcome measures were completion time for Trails A/B, total correct for Stroop sub-tasks (Stroop-W, Stroop-C, Stroop-CW) and interference score (Stroop-I) for Stroop performance, number of trials attempted and correct for PASAT, and processing time for UFOV sub-tasks (Divided Attention, Selective Attention).

Vision Measures. Visual function was assessed to rule out sensory contributions to behavioral and electrophysiological outcome measures. Early Treatment Diabetic Retinopathy Study (ETDRS) chart readings were performed with an illuminator cabinet (Precision Vision, La Salle, IL, USA) at a distance of 4 m. Visual acuity and contrast sensitivity (5%, 2.5%) was scored as the logarithm of the minimum angle of resolution.

Depression Status. Depression status was assessed using the Beck Depression Inventory (BDI), a clinical questionnaire used to assess the severity of depression symptoms (Beck and Steer,

1984; Beck et al., 1988). BDI scores range from 0 to 21, where higher scores correspond to more severe depression symptoms.

2.3. Stimulus displays and procedures

Participants were seated at an eye-to-screen distance of 58 cm from the stimulus presentation display. Stimulus displays (Fig. 1) were created in MATLab using the Psychophysics Toolbox (Brainard, 1997; Pelli, 1997). Stimulus dimensions are given in degrees of visual angle (°) and stimulus colors are given in RGB (red, green, blue[1]) values.

2.3.1. Visual search task

Participants completed a modified visual search task (Folk et al., 1992; Harris et al., 2017). Each stimulus display contained four placeholders (1.7° × 1.7°; 0.1° line thickness) subtending 3.6° from a black (0, 0, 0) central fixation dot (diameter = 0.4°), and were rendered against a gray (128, 128, 128) background. Placeholders were fixed at uniformly separated locations centered in each quadrant. In task-irrelevant cue displays, a set of four dots (diameter = 0.2°) were presented at fixed locations around each placeholder, each subtending 1.0° center-to-corner for each placeholder. In search displays, four Landolt squares (1.0° × 1.0°), each with 0.15° line thickness and 0.6° gap size, were centered in each placeholder. For each search display, Landolt square color (red [256, 0, 0], green [0, 256, 0], blue [0, 0, 256], yellow [256, 256, 0]), orientation (0°, 90°, 180°, 270°), and placeholder assignment were randomly sampled without replacement.

Task procedures for a given trial are depicted in Fig. 1A. Prior to beginning the experiment, participants were assigned a target color (e.g., red). Each trial started with a blank placeholder display for a variable inter-stimulus interval (ITI). ITI values were randomly sampled from a uniform distribution ranging from 750 to 1500 ms in increments of 50 ms. Next, the task-irrelevant cue display was presented for 50 ms. For a given trial, one of three possible cue conditions were rendered: (1) Neutral (50% of trials): All placeholder dots were rendered in black; (2) Low-Similarity (25% of trials): One set of placeholder dots were rendered in a non-target color (e.g., green, blue, yellow); and (3) High-Similarity (25% of trials): One set of placeholder dots were rendered in the target color (e.g., red). Cue and search displays were separated by a blank stimulus-onset asynchrony (SOA) display for a randomly sampled duration of 50, 150, 250, or 350 ms. Following the blank SOA display, the search display was presented until participants responded with a button press. Participants pressed either the up, down, left, or right array keys when the target orientation was 0°, 180°, 270°, or 90°, respectively.

Participants completed a total of 256 trials in approximately 10 min. The following conditions were counterbalanced across trials: cue condition, cue location, SOA duration, target location, and target orientation. Experimenters instructed participants to maintain fixation and refrain from initiating blinks or eye movements to the best of their abilities (see EEG procedures below). Experimenters instructed participants to respond as quickly and accurately as possible.

Response time (RT) was the primary behavioral outcome measure. For each trial, RT was measured as the temporal delay between the onset of task-relevant stimulus display and button press. Aggregate RT distributions were inspected individually for each participant. Incorrect trials and trials containing RT values more than 3 standard deviations greater than the mean of aggregate RT distributions were removed from further analysis. The remaining RT values were then binned and averaged for each cue condition. Normalized RT costs (d') were calculated to estimate the effect of cue condition on performance: $d' = [(X_{(a)} - X_{(b)})/\sigma_{(ab)}]$, where a and b are different cue conditions, X is average RT, and σ is pooled standard deviation of RT values across both a and b. Whereas previous studies examined only the magnitude of the difference in RT values across conditions (Harris et al., 2017), we favored the normalization method because it takes into account between-subject differences in RT variability. To assess speed-accuracy trade-offs in visual search performance, we also assessed response accuracy, which was greater than 90% across all study participants and conditions.

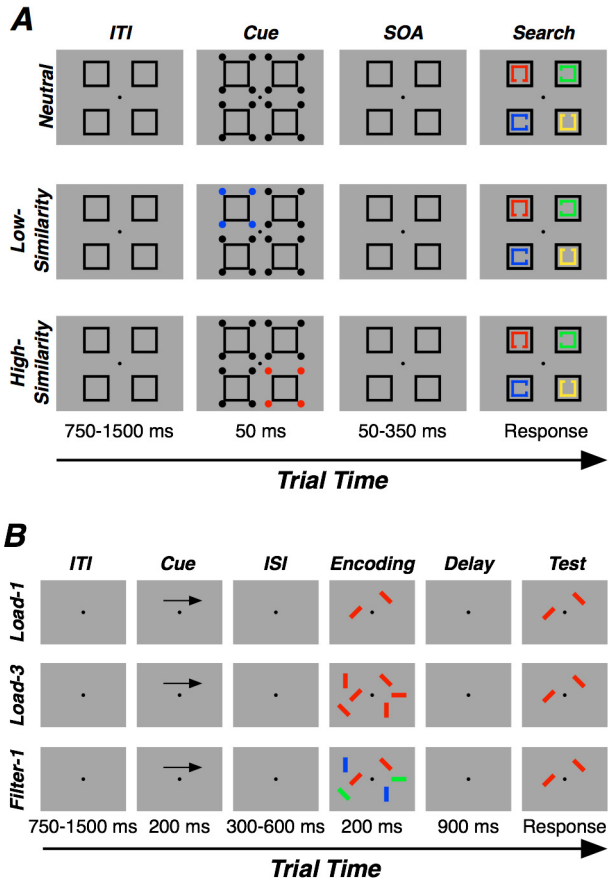

Fig. 1. Task Schematics. (A) Visual Search Task. Each trial started with an inter-trial interval (ITI) that contained four stimulus placeholders. Next, one of three cue displays were presented: (1) on 50% of trials, each placeholder was flanked by a set of black dots (neutral condition); (2) on 25% of trials, one random placeholder was flanked by a non-target colored dot (low-similarity condition); (3) on 25% of trials, one random placeholder was flanked by a target colored dot (high-similarity condition). Following a blank stimulus onset asynchrony (SOA) display, participants were instructed to respond with the direction of a red Landolt C stimulus that could be presented in one of four locations within the Search Display. **(B) Change Detection Task.** Each trial started with a blank ITI, followed by a spatial cue to attend either the left (50% of trials) or right (50% of trials) visual hemifield. Next, a blank ISI period was followed by the memory encoding display. Each trial contained either one or three red target memory items, and zero or two non-red distractor items. On a given trial, one of four conditions was presented with equal probability: (1) one red item with zero distractor items (Load-1 condition); (2) three red items with zero distractor items (Load-3 condition); (3) one red item with two distractor items (Filter-1 condition); and (4) three red items with two distractor items (Filter-3 condition; not shown in figure). Stimulus conditions were matched across hemifields, and patients were instructed to remember the cued items. Following a blank delay period, participants were presented with the test display.

2.3.2. Change detection task

Participants completed a modified change detection task (Luck and Vogel, 1997; Vogel et al., 2005). Each stimulus display con-

[1] For interpretation of color in Fig. 1, the reader is referred to the web version of this article.

tained a central black fixation dot (diameter = 0.4°) presented against a gray [128, 128, 128] background. Cue displays contained a black arrow (1.1° × 3.3°) that was oriented towards the left or right side of fixation. Memory displays contained rectangular stimuli (0.6° × 1.7°) that varied in number and color. Target items were red [256, 0, 0], and distractor items, when present, were blue [0, 0, 256] or green [0, 256, 0]. Target number (1 item, 3 items) and distractor number (0 items, 2 items) were counterbalanced, producing four total stimulus conditions: (1) Load-1: one red target item and no distractor items; (2) Load-3: three red target items and no distractor items; (3) Filter-1: one red target item and two distractor items; and (4) Filter-3: three red target items and two distractor items. Two sets of task stimuli were presented; one set was presented to the left of fixation and one set was presented to the right of fixation. Stimulus locations were constrained to areas outside of a central region (13.1° × 8.2°) and within a larger peripheral region (13.1° × 16.3°) centered over fixation. Center-to-center distances between each stimulus were greater than 2.4°. Each set of stimulus orientations were randomly oriented at 0°, 45°, 90°, or 135°, with the constraint that no two target items were the same orientation and no more than two total items were the same orientation. For test displays, a single red test stimulus was presented in a randomly sampled target location. Test stimulus orientations were either the same or different with respect to the orientation of the probed target item presented in the same location during memory displays.

Task procedures for a given trial are depicted in Fig. 1B. Participants were instructed to remember the orientation of each red target item presented within the cued side of fixation. Each trial started with a blank display for a variable ITI that was randomly sampled from a uniform distribution ranging from 750 ms to 1500 ms in increments of 50 ms. Next, a cue display was presented for 200 ms to indicate which hemifield would be tested. For trials in which the cue was oriented to the left (or right) side of fixation, participants were instructed to remember the left (or right) target items. Next, a blank display was presented for variable ISI that was randomly sampled from a uniform distribution ranging from 300 to 600 ms in increments of 100 ms. Blank ISI displays were followed by a 200 ms memory display. Following a 900 ms blank display, a test display was presented until a response was made. Participants responded by pressing the "z" or "/" key when test and probed stimulus orientations were different or the same, respectively.

Participants completed a total of 256 trials in approximately 20 min. The following conditions were counterbalanced across trials: cue orientation, target number, distractor number, and test stimulus orientation. Experimenters instructed participants to maintain fixation and refrain from initiating blinks or eye movements to the best of their abilities (see EEG procedures below). Experimenters instructed participants to respond as accurately as possible.

Response accuracy, estimated as the proportion of trials in which a correct response was made, was the primary behavioral outcome measure. For each condition, accuracy measures were binned across trials and averaged. *Load effects* on behavioral performance were estimated by dividing the difference in response accuracy between Load-1 and Load-3 conditions by the sum of response accuracy across the same conditions. *Filter effects* on behavioral performance were estimated by dividing the difference in response accuracy between Load-1 and Filter-1 conditions by the sum of response accuracy across the same conditions. Load effects and filter effects reflect weighted reductions in response accuracy associated with storing additional relevant and irrelevant items, respectively.

2.4. EEG acquisition and analysis

EEG was recorded using a NuAmps (Compumedics Neuroscan Inc., Charlotte, NC, USA) digital amplifier and silver-chloride electrodes distributed in a fitted elastic cap according to the International 10–20 System. EEG was measured from eight scalp electrodes (O1, O2, PO1, PO2, P3, P4, P7, P8) and two mastoid electrodes (A1, A2), with a ground reference electrode at the AFz site. Electrooculography (EOG) was recorded using a bipolar montage. Horizontal EOG (HEOG) was recorded from electrodes placed 1 cm outside the lateral canthus of each eye to measure eye movements; vertical EOG (VEOG) was recorded from electrodes placed above and below the left eye to measure blinks. Impedances of all electrodes were maintained below 10 kΩ. EEG signals were digitized at a sampling rate of 1000 Hz and re-referenced offline to mathematically averaged left and right mastoids (A1–A2). Stimulus event triggers were sent to the EEG amplifier through the parallel port of a dedicated stimulus presentation computer. Continuous EEG measurements were recorded and monitored on a dedicated acquisition laptop. Timing delays between stimulus presentation and event triggers were measured using an analog photometer and corrected during analysis.

EEG recordings were analyzed using EEGLab (Delorme and Makeig, 2004) and ERPLab (Lopez-Calderon and Luck, 2014) MATLAB toolboxes. EEG recordings were high-pass-filtered (0.01 Hz) and low-pass-filtered (30 Hz) using a second-order Butterworth filter. Artifact detection routines marked continuous EEG segments contaminated by blinks or eye movements in VEOG or HEOG recordings, respectively. Blinks were detected when VEOG peak-to-peak amplitude exceeded 100 μV within a 200 ms sliding window and 50 ms step size. Eye movements were detected when the absolute difference between HEOG amplitude exceeded 100 μV within a 400 ms sliding window with 10 ms step size. EEG segments containing artifacts were removed from further analysis. For the visual search task, 9.3% of all trials across groups were rejected, with 10.0% and 8.3% of trials rejected in hematologic cancer and healthy control groups, respectively. For the change detection task, 16.1% of all trials across groups were rejected, with 17.9% and 13.4% of trials rejected in hematologic cancer and healthy control groups, respectively. Due to the limited number of trials afforded by time constraints, trials were not rejected based on incorrect responses.

ERP epochs were extracted after the presentation of each stimulus display with a pre-stimulus baseline period of 200 ms. Contralateral (or ipsilateral) waveforms were created by averaging ERP epochs from right electrodes (e.g., O2, PO2, P4, P8) when the stimulus cue was presented in the left (or right) visual hemifield, and from left electrodes (e.g., O1, PO1, P3, P7) when the stimulus cue was presented in the right (or left) visual hemifield. Difference waveforms were created for each electrode pair (O1/O2, PO1/PO2, P3/P4, P7/P8) by subtracting ipsilateral waveforms from contralateral waveforms. Difference waveforms were visually inspected across all electrodes pairs.

For the visual search task, ERP waveforms were measured in PO1/PO2 and O1/O2 electrode pairs and inspected 0–400 ms after cue display onset to determine the presence of N2pc activity. N2pc amplitudes were measured within a 50 ms window between 200 ms and 350 ms after cue onset. For the change detection task, ERP waveforms were measured in PO1/PO2 and P3/P4 electrode pairs and inspected 0–1000 ms after memory display onset to determine the presence of CDA activity. CDA amplitudes were measured by averaging ERP activity from 400 to 1000 ms following memory display onset. To estimate effects of increasing storage load on CDA amplitude, we calculated CDA_{Load} as Load-3 CDA

amplitudes minus Load-1 CDA amplitudes, where larger CDA_{Load} values reflect larger load-dependent increases in CDA amplitude. To estimate effects of increasing distractor load on CDA amplitude, we calculated CDA_{Filter} as Filter-1 CDA amplitudes minus Load-1 CDA amplitudes, where larger CDA_{Filter} values reflect larger filter-related increases in CDA amplitude.

2.5. Statistical analysis

Ctx+ and Ctx− patients were combined into one group comprised of untreated patients, resulting in a patient group (Ctx+/Ctx−) and control group (HC). Analyses were performed with SAS Studio 3.6 (SAS Institute Inc.). Categorical data were descriptively summarized using frequency and percentage tables, and numeric data were descriptively summarized using means and standard deviations. Univariate graphs were created for predictor (i.e., age, education) and response variables (e.g., ERP amplitude, RT) to investigate distributional properties. Statistical significance was set to the standard $p < .05$ level. Between-group differences in demographic characteristics, vision, and depression status were assessed using chi-squared tests (PROC FREQ) for categorical variables (e.g. gender) and t-tests (PROC TTEST) for numeric variables (e.g. age).

Statistical analyses for task performance and ERP measures were performed as follows. First, we used dependent-samples t-tests to evaluate differences between task conditions across all study participants. For the visual search task, response times in low- and high-similarity conditions were compared against response times during neutral conditions, and N2pc amplitudes were compared between low- and high-similarity conditions. For the change detection task, response accuracy in the Load-3 and Filter-1 conditions were compared against response accuracy in the Load-1 condition, and similar comparisons were made for CDA amplitudes. Next, we used dependent-samples t-tests to evaluate differences between task conditions separately for each group to determine whether effects of task conditions were consistent across groups. Finally, between-group differences in each outcome measure were assessed using independent-samples t-tests; Welch-Satterthwaite t-tests were used when variance was unequal between groups. Standardized effect sizes (Cohen's d) were calculated as the between-group mean difference divided by pooled standard deviation according to PROC TTEST output. We reported those standardized effect sizes for between-group differences that exceeded a medium effect size of 0.5.

3. Results

3.1. Study sample

This work is part of a broader study aimed at measuring longitudinal changes in cognitive function in hematologic cancer patients receiving chemotherapy, and comparing those changes against comparison groups comprised of cancer patients not scheduled to receive chemotherapy and healthy controls. A total of 45 subjects were enrolled in the study. Ctx+ and Ctx− groups were comprised of heterogeneous hematologic cancer diagnoses (Table 1). Ctx+ (n = 15) patients were recruited a median of 11 days after diagnosis (range: 0–125 days); longer delays between diagnosis and chemotherapy initiation were seen in low-grade non-Hodgkin lymphoma (NHL) patients who were initially under active surveillance. Ctx− (n = 15) patients were recruited a median of 11.6 months after diagnosis (range: 0–70.1 months). One Ctx + and one Ctx- patient withdrew from the study prior to completing testing.

Table 1
Study Sample Characteristics. Study groups were demographically matched on age (mean ± SD), gender (N (%)), and education (mean ± SD). Patients were primarily diagnosed with NHL and MDS. (NHL = non-Hodgkin lymphoma; MDS = myelodysplastic syndrome; AML = acute myeloid leukemia; CLL = chronic lymphocytic leukemia; ALL = acute lymphocytic leukemia; MM = multiple myeloma).

Characteristic	Patients	Controls
Demographics	(n = 28)	(n = 15)
Age (years)	60.9 ± 13.5	60.0 ± 16.8
Gender (% males)	13 (46%)	7 (47%)
Education (years)	13.7 ± 1.5	14.3 ± 1.6
Diagnoses		
NHL	15 (53%)	
MDS	6 (21%)	
AML	3 (11%)	
CLL	2 (7%)	
ALL	1 (4%)	
MM	1 (4%)	

Study participants were prescribed an average of 3 medications, and polypharmacy (≥4 medications) was noted in 47% of Ctx+ patients, 47% of Ctx− patients, and 40% of HC participants. Medications were further evaluated to determine the frequency at which study participants were prescribed medications known to alter brain and cognitive function (e.g. anti-convulsants, opioids, corticosteroids, neurotransmitter antagonists, sedatives). Approximately 47% of patients in both Ctx+ and Ctx− groups were taking at least one of these medications, compared to only 20% of HC participants; and approximately 27% of Ctx+ patients, 20% Ctx− patients, and 7% of HC participants were taking at least two of these medications.

For the purposes of this work, which aimed to evaluate differences between untreated hematologic cancer patients and healthy comparisons, Ctx+ and Ctx− patients were combined into one group comprised of untreated patients. Some patients were unable to complete all assessments (see Tables 2–4 for sample sizes in each outcome measure). Five hematologic cancer patients completed neuropsychological assessments only. One colorblind hematologic cancer patient failed to complete Stroop-C and Stroop-CW. One hematologic cancer patient could not complete neurophysiological recordings due to lack of cap availability.

3.2. Demographics

Demographic characteristics of the complete study sample are summarized in Table 1. Study groups were balanced across demographic factors in age ($t_{(41)} = 0.19$, $p = .85$), gender ($\chi^2_{(1)} = 0.0002$, $p = 0.99$), and education ($t_{(40)} = -1.13$, $p = 0.27$).

3.3. Clinical assessment

Descriptive statistics for neuropsychological assessments are provided in Table 2. Between-group differences in neuropsychological assessments were marginally significant for Stroop-CW ($t_{(40)} = -1.55$, $p = .13$; Cohen's d = 0.59) and PASAT Attempts ($t_{(36)} = -1.85$, $p = .073$; Cohen's d = 0.62). There were no between-group differences detected in visual acuity ($t_{(36)} = 0.45$, $p = .66$) and contrast sensitivity using 5% ($t_{(36)} = 0.80$, $p = .43$) and 2.5% ($t_{(36)} = 0.75$, $p = .46$) ETDRS charts. There were no between-group differences detected in depression symptoms ($t_{(34)} = 0.96$, p = .34).

3.4. Visual search task

3.4.1. Behavior

Descriptive statistics for visual search task measures are summarized in Table 3. We first examined the effect of low- and

Table 2
Clinical Assessments of Cognitive and Visual Function. M ± SD for each outcome measure. (Stroop-W = Stroop Word Subscale; Stroop-C = Stroop Color Subscale; Stroop-CW = Stroop Color Word Subscale; Stroop-I = Stroop Interference score; PASAT = Paced Auditory Serial Addition Task; UFOV = Useful Field of View; BDI = Beck Depression Inventory) ($^{\ddagger}p < .10$).

Characteristic	All	Patients	Controls
Cognitive Assessment			
Trails A	29.3 ± 11.6 (n = 43)	29.7 ± 11.9 (n = 28)	28.5 ± 11.5 (n = 15)
Trails B	77.5 ± 51.9 (n = 43)	82.0 ± 58.1 (n = 28)	69.0 ± 38.3 (n = 15)
Stroop-W	92.7 ± 14.5 (n = 43)	91.2 ± 12.7 (n = 28)	95.5 ± 17.5 (n = 15)
Stroop-C	69.1 ± 13.9 (n = 42)	67.8 ± 14.0 (n = 27)	71.5 ± 13.7 (n = 15)
Stroop-CW‡	33.0 ± 12.9 (n = 42)	30.7 ± 11.8 (n = 27)	37.1 ± 14.0 (n = 15)
Stroop-I	6.3 ± 11.0 (n = 42)	7.9 ± 10.7 (n = 27)	3.6 ± 11.4 (n = 15)
PASAT—Correct‡	24.1 ± 7.1 (n = 38)	22.4 ± 5.9 (n = 23)	26.6 ± 8.1 (n = 15)
PASAT—Attempts‡	21.5 ± 7.4 (n = 38)	20.0 ± 6.3 (n = 23)	23.9 ± 8.5 (n = 15)
UFOV—Divided	63.3 ± 98.4 (n = 38)	66.9 ± 111.8 (n = 23)	58.0 ± 78.2 (n = 15)
UFOV—Selective	142.4 ± 107.8 (n = 38)	151.0 ± 102.3 (n = 23)	129.9 ± 117.9 (n = 15)
Vision Assessment	(n = 38)	(n = 23)	(n = 15)
100% (Acuity)	−0.06±0.09	−0.05±0.10	−0.07±0.07
5% (Contrast)	0.23±0.13	0.25±0.14	0.21±0.12
2.5% (Contrast)	0.38±0.17	0.40±0.18	0.35±0.14
Depression Status	(n = 36)	(n = 21)	(n = 15)
BDI	6.8 ± 1.1	8.2 ± 6.0	6.0 ± 7.7

Table 3
Visual Search Task Outcome Measures. M ± SD for each outcome measure. (RT = response time; d′ = response time cost). ($^{*}p < .05$; $^{**}p < .001$).

Measure	All	Patients	Controls
Behavior	(n = 38)	(n = 23)	(n = 15)
Neutral Accuracy	0.99 ± 0.01	0.99 ± 0.02	0.99 ± 0.01
Low-similarity Accuracy	0.99 ± 0.02	0.98 ± 0.02	0.99 ± 0.01
High-similarity Accuracy	0.99 ± 0.02	0.99 ± 0.02	0.99 ± 0.02
Neutral RT	860 ± 166	838 ± 139	895 ± 201
Low-similarity RT	846 ± 167	828 ± 144	874 ± 199
High-similarity RT	896 ± 169	867 ± 145	939 ± 199
Low-similarity d'	−0.08 ± 0.14	−0.06 ± 0.13	−0.10 ± 0.15
High-similarity d'	0.19 ± 0.17	0.17 ± 0.18	0.22 ± 0.16
Electrophysiology	(n = 37)	(n = 22)	(n = 15)
Low-similarity N2pc*	−0.23 ± 0.64	−0.44 ± 0.73	0.08 ± 0.28
High-similarity N2pc**	−0.73 ± 0.77	−0.92 ± 0.88	−0.45 ± 0.49

Table 4
Change Detection Task Outcome Measures. M ± SD for each outcome measure. (CDA = contralateral delay activity).

Measure	All	Patients	Controls
Behavior	(n = 36)	(n = 22)	(n = 14)
Load-1 Accuracy	0.89 ± 0.10	0.89 ± 0.08	0.89 ± 0.12
Load-3 Accuracy	0.67 ± 0.11	0.65 ± 0.09	0.70 ± 0.13
Filter-1 Accuracy	0.88 ± 0.09	0.89 ± 0.07	0.88 ± 0.12
Filter-3 Accuracy	0.64 ± 0.10	0.62 ± 0.09	0.67 ± 0.11
Load Effect	0.14 ± 0.06	0.16 ± 0.05	0.12 ± 0.07
Filter Effect	0.004 ± 0.02	0.002 ± 0.02	0.006 ± 0.02
Electrophysiology	(n = 34)	(n = 20)	(n = 14)
Load-1 CDA	−0.12 ± 0.44	−0.05 ± 0.41	−0.21 ± 0.47
Load-3 CDA	−0.85 ± 0.67	−0.79 ± 0.72	−0.92 ± 0.60
Filter-1 CDA	−0.30 ± 0.32	−0.32 ± 0.35	−0.27 ± 0.27
Filter-3 CDA	−0.80 ± 0.63	−0.78 ± 0.62	−0.83 ± 0.66
CDA_{Load}	−0.73 ± 0.76	−0.74 ± 0.76	−0.71 ± 0.78
CDA_{Filter}	−0.18 ± 0.50	−0.27 ± 0.50	−0.06 ± 0.21

high-similarity cues on visual search performance. RTs were faster during low-similarity trials ($t_{(37)} = 3.34$, $p = .0019$) and slower during high-similarity trials ($t_{(37)} = -6.73$, $p < .0001$) compared to neutral trials. Similarly, non-zero d' estimates were observed for both low-similarity ($t_{(37)} = -3.59$, $p = .0009$; Cohen's d = 1.2) and high-similarity ($t_{(37)} = 6.86$, $p < .0001$; Cohen's d = 2.3) conditions. These results support previous work demonstrating an effect of cue-target similarity on visual search performance (Harris et al., 2017).

We next evaluated group differences in visual search outcome measures. Hematologic cancer and healthy control groups showed non-zero d' estimates for both low-similarity (hematologic cancer: $t_{(22)} = -2.38$, $p = .026$; healthy control: $t_{(14)} = -2.69$, $p = .018$) and high-similarity (hematologic cancer: $t_{(22)} = 4.52$, $p = .0002$; healthy control: $t_{(14)} = 5.48$, $p < .0001$) conditions. We failed to detect between-group differences in d' estimates for low-similarity ($t_{(36)} = 0.89$, $p = .38$) and high-similarity ($t_{(36)} = 0.99$, $p = .33$) conditions. We further failed to detect between-group differences in RT during neutral ($t_{(36)} = -1.03$, $p = .31$), low-similarity ($t_{(36)} = -0.82$, $p = .42$), and high-similarity trials ($t_{(36)} = -1.29$, $p = 0.21$). These results indicate visual search performance was similar between hematologic cancer and healthy control groups.

3.4.2. Electrophysiology

Collapsing across groups, ERP waveforms (Fig. 2) revealed a larger negativity in contralateral compared to ipsilateral electrodes approximately 200 ms following cue onset during low-similarity (Fig. 2A) and high-similarity (Fig. 2B) trials. Mean N2pc amplitudes were measured 230–280 (255 ± 25) ms following cue onset (Table 3). We observed a greater contralateral negativity during the N2pc window in both low-similarity ($t_{(36)} = -2.22$, $p = .033$) and high-similarity ($t_{(36)} = -5.73$, $p < .0001$) conditions, demonstrating evidence for reliable N2pc activity. Difference waveforms were created by subtracting ipsilateral from contralateral activity. We observed a large negative deflection in ERP amplitude consistent with the N2pc component (Fig. 2C). Larger N2pc amplitudes were observed during high-similarity relative to low-similarity trials ($t_{(36)} = 7.27$, $p < .0001$). These results support previous work demonstrating larger N2pc amplitudes during high-similarity relative to low-similarity cue conditions (Harris et al., 2017).

ERP amplitudes were evaluated separately for hematologic cancer and healthy control groups (Table 3). In the hematologic cancer group, we observed a greater contralateral negativity during the N2pc window in both low-similarity ($t_{(21)} = -2.85$, $p = .0096$) and high-similarity ($t_{(21)} = -4.93$, $p < .0001$) conditions. In the healthy control group, we observed a greater contralateral negativity during the N2pc window in high-similarity ($t_{(14)} = -3.53$, $p = .0033$), but not low-similarity ($t_{(14)} = 1.03$, $p = .33$), conditions. Between-group differences in N2pc amplitude were detected for both low-similarity ($t_{(29.2)} = -3.01$, $p = .0053$; Cohen's d = 1.12) and high-similarity ($t_{(33.9)} = -2.11$, $p = .042$; Cohen's d = 0.72) trials. These results demonstrate N2pc amplitudes were larger in hematologic cancer patients relative to healthy controls in both low- and high-similarity cue conditions.

3.5. Change detection task

3.5.1. Behavior

Descriptive statistics for change detection task measures are summarized in Table 4. Response accuracy was lower during Load-3 trials ($t_{(35)} = 14.92$, $p < .0001$; Cohen's d = 5.0), but not Filter-1 trials ($t_{(35)} = 1.15$, $p = .26$), compared to Load-1 trials. Similarly, we observed non-zero load effects ($t_{(35)} = 13.6$, $p < .0001$), but failed to observe non-zero filter effects ($t_{(35)} = 1.16$, $p = .25$). These results mirror a previous study in older adults (Jost et al., 2011), which support well-established load effects but failed to observe filter effects on change detection response accuracy.

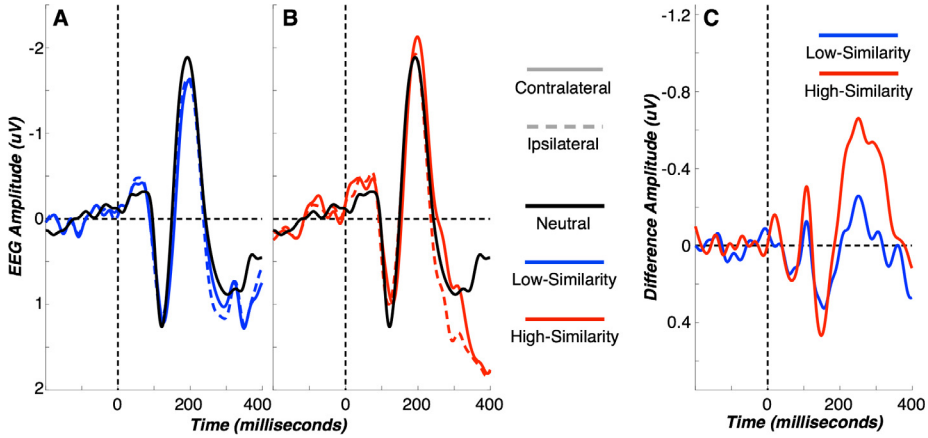

Fig. 2. Visual Search Task: ERPs. EEG recordings were time-locked to task-irrelevant cue onset. **(A, B)** Contralateral (solid lines) and ipsilateral (dashed lines) waveforms are shown collapsed across groups (n = 37) for low-similarity (**A**; blue lines) and high-similarity (**B**; red lines) conditions. Amplitude differences between contralateral and ipsilateral waveforms are apparent approximately 200 ms after cue display onset, consistent with N2pc activity. Neutral waveforms (solid black) are plotted for comparison in both **A** and **B**. **(C)** Difference waveforms were created by subtracting ipsilateral from contralateral waveforms. N2pc activity emerged approximately 200 ms after cue display onset for both low-similarity ($p = .033$) and high-similarity ($p < .0001$) conditions. Larger N2pc amplitudes were observed in high-similarity (red) relative to low-similarity (blue) trials ($p < .0001$). (For interpretation of the references to colour in this figure legend, the reader is referred to the web version of this article.)

We next examined group differences in change detection outcome measures. Both hematologic cancer ($t_{(21)} = 13.73$, $p < .0001$; Cohen's d = 6.0) and healthy control ($t_{(13)} = 6.35$, $p < .0001$; Cohen's d = 3.5) groups showed reliable Load effects, demonstrating robust storage load costs between groups. Furthermore, we observed a relatively larger Load Effect in the hematologic cancer group compared to the healthy control group ($t_{(34)} = 1.99$, $p = .054$; Cohen's d = 0.68). In contrast, we failed to detect reliable filter effects in both hematologic cancer ($t_{(21)} = 0.58$, $p = .57$) and healthy control groups ($t_{(13)} = 1.12$, $p = .29$), and also failed to detect between-group effects on filter effects ($t_{(34)} = -0.53$, $p = .60$). Furthermore, we failed to detect between-group differences in response accuracy during Load-1 ($t_{(34)} = 0.28$, $p = .78$), Filter-1 ($t_{(19.18)} = 0.41$, p = .69), Load-3 ($t_{(34)} = -1.38$, $p = .18$), and Filter-3 ($t_{(34)} = -1.48$, $p = .15$) conditions. These results indicate hematologic cancer patients showed larger reductions in change detection performance relative to healthy controls as working memory storage load increased, whereas both groups showed similar changes in change detection performance as distractor load increased.

3.5.2. Electrophysiology

ERP waveforms revealed a larger negativity in contralateral compared to ipsilateral electrodes that emerged approximately 300 ms following memory display onset (Fig. 3A–C). Mean CDA amplitudes were measured 400–1000 ms following memory display onset (Table 4). We observed a greater contralateral negativity during the CDA window in the Load-3 ($t_{(33)} = -7.36$, $p < .0001$; Fig. 3C), Filter-1 ($t_{(33)} = -5.49$, $p < .0001$; Fig. 3B), and Filter-3 ($t_{(33)} = -7.46$, $p < .0001$) conditions; we failed to observe a greater negativity during the Load-1 condition ($t_{(33)} = -1.57$, $p = .13$; Fig. 3A). Difference waveforms were created by subtracting ipsilateral from contralateral activity, revealing a sustained negativity in ERP amplitude consistent with the CDA component (Fig. 3D). Larger CDA amplitudes were observed during both Load-3 ($t_{(33)} = 5.62$, $p < .0001$; Cohen's d = 1.96) and Filter-1 ($t_{(33)} = 2.15$, $p = .039$; Cohen's d = 0.75) conditions compared to the Load-1 condition. Finally, waveforms demonstrating load effects and filter effects were created by subtracting Load-1 difference waveforms from Load-3 and Filter-1 difference waveforms, respectively (Fig. 3E). These results support previous studies showing greater storage-related neurophysiological activity as storage load and filter demands increase (Jost et al., 2011; Vogel et al., 2005).

Next, ERP amplitudes were evaluated separately for hematologic cancer and healthy control groups (Table 4). In the hematologic cancer group, we observed a greater contralateral negativity during the CDA window in the Load-3 ($t_{(19)} = -4.90$, $p < .0001$), Filter-1 ($t_{(19)} = -4.02$, $p = .0007$), and Filter-3 ($t_{(19)} = -5.68$, $p < .0001$) conditions; we failed to observe a greater negativity in the Load-1 condition ($t_{(19)} = -0.55$, $p = .59$). In the healthy control group, we observed a greater contralateral negativity during the CDA window in the Load-3 ($t_{(13)} = -5.72$, $p < .0001$), Filter-1 ($t_{(13)} = -3.79$, $p = .0023$), and Filter-3 ($t_{(13)} = -4.67$, $p = .0004$) conditions; we failed to observe a greater contralateral negativity in the Load-1 condition ($t_{(13)} = -1.69$, $p = .11$). Both hematologic cancer ($t_{(19)} = -4.37$, $p = .0003$; Cohen's d = 2.0) and healthy control ($t_{(13)} = -3.41$, $p = .0046$; Cohen's d = 1.89) groups showed non-zero CDA_{Load} amplitudes, demonstrating robust increases in storage-related neurophysiological activity across groups. In contrast, we failed to detect between-group effects on CDA_{Load} amplitudes ($t_{(32)} = -0.12$, $p = .90$). Non-zero CDA_{Filter} amplitudes were observed in the hematologic cancer group ($t_{(19)} = -2.37$, $p = .028$; Cohen's d = 1.1), but not in the healthy control group ($t_{(13)} = -0.48$, p = .64). Furthermore, we failed to detect between-group effects on CDA_{Filter} amplitudes ($t_{(32)} = -1.21$, $p = .24$). These results indicate hematologic cancer patients, but not healthy controls, showed an increase in CDA amplitude as distractor load increased in memory displays. In contrast, hematologic cancer patients and healthy controls showed similar increases in CDA amplitude as working memory storage load increased in memory displays.

4. Discussion

In this work, we found novel neurophysiological evidence that indicates untreated hematologic cancer patients, in comparison to healthy controls, are impaired in controlling spatial shifts of attention and manipulating information in working memory. Importantly, differences between hematologic cancer patients and healthy controls could not be explained by differences in age, gender, education, or visual function. Our findings complement previous PET studies of hematologic cancer patients that demonstrated altered metabolic brain activity in dorsal attention and central executive networks (Baudino et al., 2012; D'Agata et al., 2013). Specifically, cognitive processes such as controlling spatial shifts of attention and manipulating information in working

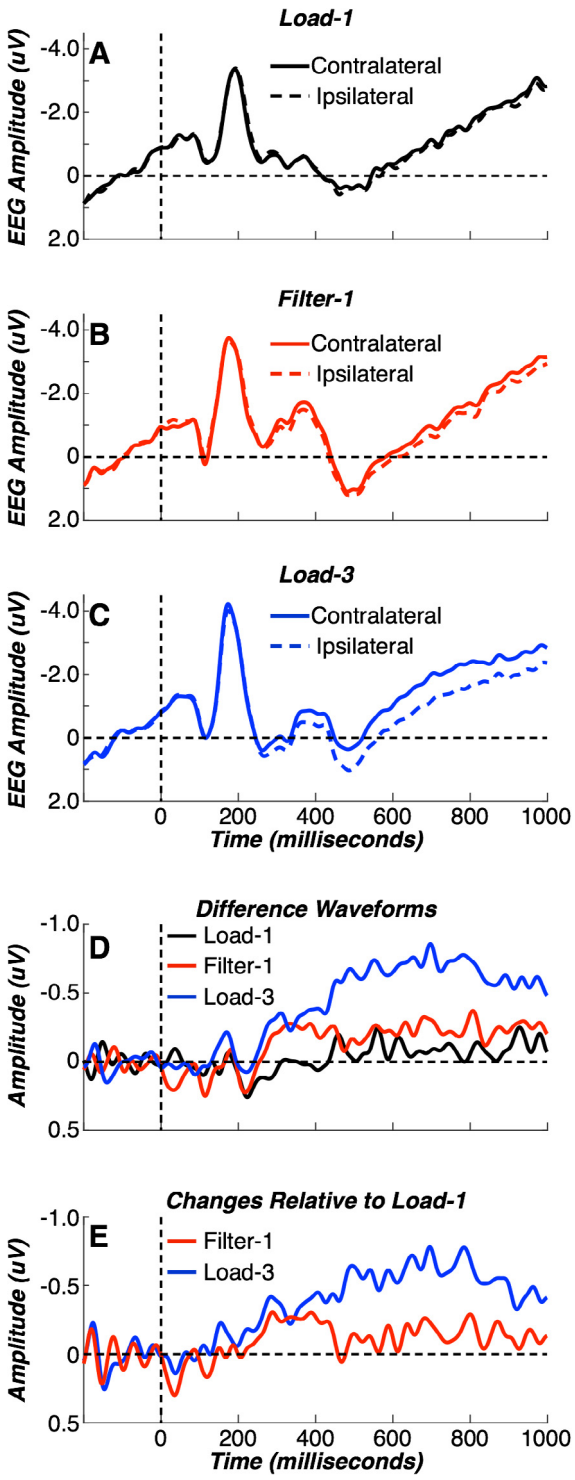

Fig. 3. Change Detection Task: ERPs. EEG recordings were time-locked to the encoding display. (**A–C**). Contralateral (solid lines) and ipsilateral (dashed lines) waveforms are shown collapsed across groups (n = 34) for Load-1 **(A)**, Filter-1 **(B)**, and Load-3 **(C)** conditions. Amplitude differences are apparent approximately 300–400 ms after encoding display onset, consistent with CDA activity. **(D)**. Differences waveforms were created by subtracting ipsilateral from contralateral waveforms. The CDA was emerged approximately 400–1000 ms after encoding display onset for Load-3 ($p < .0001$; blue line) and Filter-1 conditions ($p < .0001$; red line), but not the Load-1 condition ($p = .13$; black line). **(E)**. Effects of storage load and distractor load on the CDA were estimated by subtracting Load-1 waveforms from Load-3 and Filter-1 waveforms, respectively. Effects of both storage load ($p < .0001$; blue line) and distractor load ($p < .05$; red line) were present in CDA amplitude. (For interpretation of the references to colour in this figure legend, the reader is referred to the web version of this article.)

memory are associated with patterns of activity within dorsal attention and central executive networks, respectively (Capotosto et al., 2009; Miller and Cohen, 2001; Müller and Knight, 2006; Ptak and Schnider, 2010). This work provides initial support for the hypothesis that brain network dysfunction may translate to poor control over attention and working memory processes in hematologic cancer patients, though much work is needed to bridge this knowledge gap.

These results contribute to a small body of literature on cognitive impairment in hematologic cancer patients studied prior to initiating treatment (Dubruille et al., 2015; Khan et al., 2016; Meyers et al., 2005). Previous studies have documented impaired performance during neuropsychological assessments of verbal memory, verbal fluency, visual attention, and processing speed (Meyers et al., 2005). The current study contributes to this literature by demonstrating neurophysiological evidence for impaired control over attention and working memory in untreated hematologic cancer patients. Our hypothesis is that impairments in control over attention and working memory may contribute to the broader patterns of cognitive impairment reported in previous studies. This hypothesis is supported by previous PET studies of hematologic cancer patients showing altered metabolic activity in dorsal attention and central executive networks associated with control over attention and working memory (Baudino et al., 2012; D'Agata et al., 2013). Further research is necessary to determine the relationship between neurophysiological measures of control over attention and working memory, dorsal attention and central executive network function, and neuropsychological performance.

Behavioral task performance was similar between hematologic cancer patients and healthy controls despite observed differences in task-related neurophysiological activity. Similar discrepancies between behavioral and neural measures have been reported in studies of cognitive aging (Reuter-Lorenz, 2002; Reuter-Lorenz and Cappell, 2008). Cognitive aging studies propose compensatory mechanisms in older adults overcome brain network dysfunction by recruiting additional brain regions during task performance. For example, age-related posterior-to-anterior shifts in topographic neurophysiological activity has been proposed to reflect additional recruitment of frontal brain areas to overcome deficits in posterior brain areas (Davis et al., 2008). Connections between empirical patterns in studies of cognitive aging and cancer-related cognitive impairment suggest similar compensatory mechanisms may contribute to observed discrepancies between behavioral and neural measures (Ahles, 2012; Janelsins et al., 2014; Maccormick, 2006). Thus, neurophysiological measures such as those reported here may be more sensitive to changes in brain function reported in hematologic cancer patients.

Depression is common among cancer patients (Caruso et al., 2017) and is often associated with cognitive dysfunction (Jamieson, et al., 2019; McDermott and Ebmeier, 2009). Consequently, we tested for depression using a well-established depression symptom inventory (Beck and Steer, 1984; Beck et al., 1988) and found no difference between hematologic cancer patients and healthy comparisons. Future studies may include formal psychiatric evaluations to assess for confounding effects of depression that might not be evident with these clinical screening tools.

There are several limitations to this study. (1) The small and heterogeneous sample size limited the power of the study. Effect sizes indicated some results, including non-significant neuropsychological findings, may be important for future study despite not reaching statistical significance. (2) This study did not correct for multiple comparisons and missing data may have introduced biases in reported results. Future large-scale confirmatory studies will be necessary to overcome these limitations. (3) This study lacked a comparison group to control for effects of stress following

a cancer diagnosis. Given that a cancer diagnosis may itself serve as a constant source of distraction, future studies may consider including additional groups to control for diagnosis-related stress. (4) The heterogeneous patient sample spanned multiple hematologic malignancies and included patients with variable time since diagnosis, limiting our ability to identify disease-specific patterns of cognitive impairment. (5) We cannot rule out contributions from other medical and psychosocial factors, such as co-morbidities, medications that affect brain and cognitive function, sleep quality, and stress/anxiety.

5. Conclusions

In conclusion, we found novel neurophysiological evidence that untreated hematologic cancer patients are impaired in controlling spatial shifts of attention and manipulating information in working memory. These results suggest hematologic cancer patients may be at a higher risk for selecting, processing, and storing distracting information that would compete with more immediate goal-related behaviors. Future studies may extend this work by: (1) focusing on more homogenous populations to elucidate disease- and treatment-specific contributions to altered neurophysiological measures; (2) linking EEG measures with other neuroimaging modalities (e.g., MRI, PET) to pinpoint cortical regions susceptible to pathophysiology of hematologic malignancies; (3) linking changes in EEG measures with concurrent changes in cognitive function following behavioral interventions (e.g. exercise, yoga, meditation).

Author contributions

D.E.A., V.R.B., and M.R. contributed to the conception and design of the study. D.E.A. and K.S. contributed to the acquisition and analysis of data. All authors contributed significantly to writing the manuscript.

Acknowledgements

We thank Andrew Alexander for his assistance with EEG analysis scripting. We thank Daniel Murman, M.D. and Diane Ehlers, Ph. D. for manuscript comments.

This study was supported by the Fred & Pamela Buffett Cancer Center Support Grant from the National Cancer Institute (P30 CA036727), National Institute on Aging R01 AG017177, Research Support Funds from the Clinical Research Center at the University of Nebraska Medical Center, and the Department of Neurological Sciences at the University of Nebraska Medical Center.

Conflict of interest

The authors declare there is no conflict of interest regarding the publication of this work.

References

Ahles TA. Brain vulnerability to chemotherapy toxicities. Psychooncology 2012;21 (11):1141–8.
Ball KK, Beard BL, Roenker DL, Miller RL, Griggs DS. Age and visual search: expanding the useful field of view. J Opt Soc Am A 1988;5(12):2210–9.
Bang OY, Seok JM, Kim SG, Hong JM, Kim HY, Lee J, et al. Ischemic stroke and cancer: stroke severely impacts cancer patients, while cancer increases the number of strokes. J Clin Neurol 2011;7(2):53.
Baudino B, D'agata F, Caroppo P, Castellano G, Cauda S, Manfredi M, et al. The chemotherapy long-term effect on cognitive functions and brain metabolism in lymphoma patients. Q J Nucl Med Mol Im 2012;56(6):559–68.
Beck AT, Steer RA. Internal consistencies of the original and revised beck depression inventory. J Clin Psychol 1984;40(6):1365–7.
Beck AT, Steer RA, Carbin MG. Psychometric properties of the Beck Depression Inventory: twenty-five years of evaluation. Clin Psychol Rev 1988;8(1):77–100.
Brainard DH. The psychophysics toolbox. Spatial Vision 1997;10(4):433–6.
Capotosto P, Babiloni C, Romani GL, Corbetta M. Frontoparietal cortex controls spatial attention through modulation of anticipatory alpha rhythms. J Neurosci 2009;29(18):5863–72.
Caruso R, Nanni MG, Riba M, Sabato S, Mitchell AJ, Croce E, Grassi L. Depressive spectrum disorders in cancer: prevalence, risk factors and screening for depression: a critical review. Acta Oncol 2017;56(2):146–55.
Corbetta M, Shulman GL. Control of goal-directed and stimulus-driven attention in the brain. Nat Rev Neurosci 2002;3(3):215–29.
D'Agata F, Costa T, Caroppo P, Baudino B, Cauda F, Manfredi M, et al. Multivariate analysis of brain metabolism reveals chemotherapy effects on prefrontal cerebellar system when related to dorsal attention network. EJNMMI Res 2013;3(1):22.
Davis SW, Dennis NA, Daselaar SM, Fleck MS, Cabeza R. Que PASA? The posterior-anterior shift in aging. Cereb Cortex 2008;18(5):1201–9.
Delorme A, Makeig S. EEGLAB: an open source toolbox for analysis of single-trial EEG dynamics including independent component analysis. J Neurosci Meth 2004;134(1):9–21.
Dubruille S, Libert Y, Roos M, Vandenbossche S, Collard A, Meuleman N, et al. Identification of clinical parameters predictive of one-year survival using two geriatric tools in clinically fit older patients with hematological malignancies: major impact of cognition. J Geriatr Oncol 2015;6(5):362–9.
Folk CL, Remington RW, Johnston JC. Involuntary covert orienting is contingent on attentional control settings. J Exp Psychol Human 1992;18(4):1030–44.
Golden C. Stroop Color and Word Test: A Manual for Clinical and Experimental Uses. Chicago, Illinois: Skoelting; 1978.
Gronwall DMA, Sampson HD. The psychological effects of concussion. Auckland University Press; 1974.
Harris AM, Dux PE, Jones CN, Mattingley JB. Distinct roles of theta and alpha oscillations in the involuntary capture of goal-directed attention. NeuroImage 2017;152:171–83.
Hshieh TT, Jung WF, Grande LJ, Chen J, Stone RM, Soiffer RJ, Abel GA. Prevalence of cognitive impairment and association with survival among older patients with hematologic cancers. JAMA Oncol 2018.
Hutchinson AD, Hosking JR, Kichenadasse G, Mattiske JK, Wilson C. Objective and subjective cognitive impairment following chemotherapy for cancer: a systematic review. Cancer Treat Rev 2012;38(7):926–34.
Jamieson A, Goodwill AM, Termine M, Campbell S, Szoeke C. Depression related cerebral pathology and its relationship with cognitive functioning: a systematic review. J Affect Disorders 2019;250:410–8.
Janelsins MC, Kesler SR, Ahles TA, Morrow GR. Prevalence, mechanisms, and management of cancer-related cognitive impairment. Int Rev Psychiatr 2014;26 (1):102–13.
Jost K, Bryck RL, Vogel EK, Mayr U. Are old adults just like low working memory young adults? Filtering efficiency and age differences in visual working memory. Cereb Cortex 2011;21(5):1147–54.
Khan MA, Garg K, Bhurani D, Agarwal NB. Early manifestation of mild cognitive impairment in B-cell non-Hodgkin's lymphoma patients receiving CHOP and rituximab-CHOP chemotherapy. N-S Arch Pharmacol 2016;389(12):1253–65.
Lezak MD. Neuropsychological assessment. Oxford University Press; 1995.
Lopez-Calderon J, Luck SJ. ERPLAB: an open-source toolbox for the analysis of event-related potentials. Front Hum Neurosci 2014;8:213.
Luck SJ, Hillyard SA. Electrophysiological correlates of feature analysis during visual search. Psychophysiology 1994;31(3):291–308.
Luck SJ, Vogel EK. The capacity of visual working memory for features and conjunctions. Nature 1997;390(6657):279–81.
Luria R, Balaban H, Awh E, Vogel EK. The contralateral delay activity as a neural measure of visual working memory. Neurosci Biobehav R 2016;62:100–8.
Maccormick RE. Possible acceleration of aging by adjuvant chemotherapy: A cause of early onset frailty? Med Hypotheses 2006;67(2):212–5.
McDermott LM, Ebmeier KP. A meta-analysis of depression severity and cognitive function. J Affect Disorders 2009;119(1–3):1–8.
Meyers CA, Albitar M, Estey E. Cognitive impairment, fatigue, and cytokine levels in patients with acute myelogenous leukemia or myelodysplastic syndrome. Cancer 2005;104(4):788–93.
Miller EK, Cohen JD. An integrative theory of prefrontal cortex function. Ann Rev Neurosci 2001;24(1):167–202.
Müller NG, Knight RT. The functional neuroanatomy of working memory: contributions of human brain lesion studies. Neuroscience 2006;139(1):51–8.
Pelli DG. The VideoToolbox software for visual psychophysics: transforming numbers into movies. Spatial Vision 1997;10(4):437–42.
Ptak R, Schnider A. The dorsal attention network mediates orienting toward behaviorally relevant stimuli in spatial neglect. J Neurosci 2010;30 (38):12557–65.
Reuter-Lorenz PA. New visions of the aging mind and brain. Trends Cogn Sci 2002;6 (9).
Reuter-Lorenz PA, Cappell KA. Neurocognitive aging and the compensation hypothesis. Curr Dir Psychol Sci 2008;17(3):177–82.
Sridharan D, Levitin DJ, Menon V. A critical role for the right fronto-insular cortex in switching between central-executive and default-mode networks. P Natl Acad Sci USA 2008;105(34):12569–74.
Theeuwes J. Stimulus-driven capture and attentional set: selective search for color and visual abrupt onsets. J Exp Psychol Human 1994;20(4):799–806.

Vogel EK, Machizawa MG. Neural activity predicts individual differences in visual working memory capacity. Nature 2004;428(6984):748–51.
Vogel EK, McCollough AW, Machizawa MG. Neural measures reveal individual differences in controlling access to working memory. Nature 2005;438 (7067):500–3.
Vossel S, Geng JJ, Fink GR. Dorsal and ventral attention systems: distinct neural circuits but collaborative roles. Neuroscientist 2014;20(2):150–9.
Williams AM, Zent CS, Janelsins MC. What is known and unknown about chemotherapy-related cognitive impairment in patients with haematological malignancies and areas of needed research. Br J Haematol 2016;174(6):835–46.
Woodman GF, Luck SJ. Electrophysiological measurement of rapid shifts of attention during visual search. Nature 1999;400(6747):867–9.